UNIVERSITY OF AMSTERDAM

UvA-DARE (Digital Academic Repository)

Converting lignin to aromatics: step by step

Strassberger, Z.I.

Publication date
2014

Link to publication

Citation for published version (APA):
Strassberger, Z. I. (2014). *Converting lignin to aromatics: step by step*. [Thesis, fully internal, Universiteit van Amsterdam].

General rights
It is not permitted to download or to forward/distribute the text or part of it without the consent of the author(s) and/or copyright holder(s), other than for strictly personal, individual use, unless the work is under an open content license (like Creative Commons).

Disclaimer/Complaints regulations
If you believe that digital publication of certain material infringes any of your rights or (privacy) interests, please let the Library know, stating your reasons. In case of a legitimate complaint, the Library will make the material inaccessible and/or remove it from the website. Please Ask the Library: https://uba.uva.nl/en/contact, or a letter to: Library of the University of Amsterdam, Secretariat, Singel 425, 1012 WP Amsterdam, The Netherlands. You will be contacted as soon as possible.

UvA-DARE is a service provided by the library of the University of Amsterdam (https://dare.uva.nl)

Download date:11 Feb 2025

Chapter 4

Catalytic cleavage of lignin β-O-4 link mimics using copper on alumina and magnesia-alumina

Abstract

Copper on γ-alumina and on mixed magnesia/alumina, Cu/MgO−Al_2O_3, catalyse the hydrodeoxygenation (HDO) of β−O−4 lignin-type dimers, giving valuable aromatics. The typical selectivity to phenol is 20%. By changing the support's acidity we can modify the dispersion of copper. Interestingly, more HDO occurs with larger copper agglomerates than with finely dispersed particles. The presence of copper also increases the selectivity of the HDO cleavage when compared to the bare support. Three different pathways are hypothesized for the reaction on the catalyst surface. We believe that copper activates ketones and, especially, more selectively towards β−O−4 cleavage than the alcoholic counterparts. DFT calculations of bond dissociation energies correlate well with this experimental observation. Excitingly, ethylbenzene is formed in proportional amounts to phenol, showing that these catalysts can reduce the oxygen content of lignin-type product streams.

Part of this work has been published as: *"Catalytic cleavage of lignin ß-O-4 link mimics using copper on alumina and magnesia-alumina."* Z. Strassberger, A.H. Alberts, M.J. Louwerse, S. Tanase and G. Rothenberg, *Green Chem.,* **2013**, 15, 768-774. The DFT simulations were done by Dr. M.J. Louwerse and are included here for clarity and completeness.

4.1. Introduction

Historically, hydrodesulfurization (HDS) and hydrodenitrogenation (HDN) reactions were first investigated to improve the catalytical sulfur and nitrogen removal in crude oil upgrading to reduce SO_x and NO_x emission gases during combustion.[1-3] In contrast to crude oil, hydrodeoxygenation (HDO) is the main reaction occurring in the hydrotreatment of biomass feedstock.[4-6] The oxygen content of biomass can vary between 10 wt% to 45 wt%, where oxygen is present in more than 300 products identified in pyrolysis oils.[7] Oxygen content is only about 2 wt% in conventional crude oil.[8] This can also be explained by the intrinsic nature of lignin. Phenylpropane monomers are the major units of lignin, linked together through C–O bonds of α- and β-arylalkyl ethers.[9-11] The β−O−4 linkages account for roughly 50% of all the linkages in lignin.[12-14] Cleaving them selectively would give smaller fragments, while preserving the aromatic groups. The difficult task is then not lignin depolymerisation, but rather finding a catalyst that will selectively cleave the β−O−4 linkages (and hydrodeoxygenate functional groups) while preserving the aromaticity. Hence, understanding HDO is essential for finding a selective catalytic alternative to convert lignin into high-value aromatics.

Hydrodeoxygenation conditions and the hydrogen consumption depend significantly on the nature of the type of oxygenated compounds.[1] Different chemical bonds have to be broken before the oxygen can be removed. The bond strength of the oxygen attached to an aromatic carbon is about 84 kJ/mol greater than the one attached to an aliphatic carbon.[1] This means that the oxygen from an aromatic group is more difficult to remove than from an aliphatic one. Simple aromatic model compounds were first studied in hydrogenolysis and hydrocracking of the carbon-oxygen bond for phenol, *o*-cresol, anisole, and guaiacol.[15, 16] Generally, hydrodeoxygenation can follow two pathways: (i) direct deoxygenation of phenolic types to aromatics or (ii) ring hydrogenation followed by deoxygenation.[16] The pathways are significantly influenced by the hydrogen pressure and working at high pressure favors the second route.[16]

The reduction of aromatic ketones and aldehydes to their corresponding alkanes is an important reaction for the chemical industry. Traditionally, the acidic Clemmensen and the basic Wolff–Kishner–Huangminlon reactions were used.[17] However, due to negative environmental impact, heterogeneous and homogeneous catalysis spread in practice.[17] An example of large scale application is the reduction of 2,3-dimethoxybenzaldehyde to 1,2-dimethoxy-toluene using Pd/C in ethyl acetate (see scheme 1).[18] The first experiments using only 5 %wt Pd/C (with 5%wt active metal), hydrogen pressure (0.3 bar) and room temperature showed a rapid conversion to the alcohol (intermediate). Full reduction to its corresponding alkane took over 48h. Doubling the catalyst loading reduced the reaction time to 15h with only 0.4% residual alcohol.

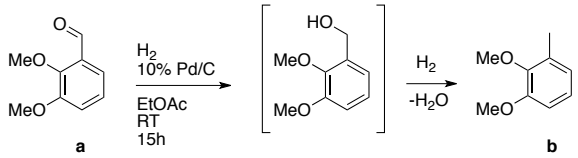

Scheme 1: Catalytic reduction of 2,3-dimethoxybenzaldehyde (**a**) to 2,3-dimethoxy-toluene (**b**).

The reduction of ketones to alkane derivatives is more common than the analogous reduction of aldehydes. Several methods are published, including the Wolff−Kishner reaction (hydrazine/KOH),[19] silicon-based reducing agents,[20] and other homogeneous systems.[21-23] Heterogeneous catalytic reactions use typically palladium[17, 24] nickel,[25] platinum[26, 27], ruthenium or copper as catalysts.[28, 29] In most cases, two main factors influence selectivity towards hydrogenation of the C=O bond versus the aromatic ring: (i) the choice of support and (ii) the crystallite size.[26] For platinum based catalysts, titania was found to be the more selective than SiO_2 and Al_2O_3.[30] In this study, bulk (unsupported) metal particles (940 nm) resulted in a higher selectivity towards cyclohexane and cyclohexanol when compared to finely dispersed supported particles (1 nm).

4.2. Catalytic cleavage of lignin β-O-4 link mimics using copper on alumina and magnesia-alumina

4.2.1. Copper catalysts in hydrodeoxygenation reactions

First, we selected appropriate β−O−4 linkage analogues. These must be similar enough to real lignin so that the results are relevant, yet still simple enough for carrying out meaningful experiments on laboratory scale. In the line of previous research focused on small monomers and alcohol-ether-type dimers,[31-33] we opted for ketone-ether dimers, which are also important products of lignin depolymerisation.[34, 35] Thus, we selected 2−phenoxy−1−phenylethanone **1** and 2−phenoxy−1−phenylethanol **2**.[36] These were synthesized following the procedure of Britt *et al*. (eqs 1 and 2).[37]

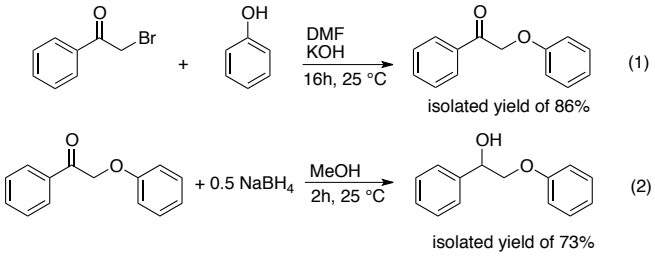

In terms of catalysts, we focused on copper and copper oxide supported on γ−Al_2O_3 and MgO−Al_2O_3. Apart from their economic and environmental advantages over noble metals,[38] copper catalysts are also reported active for hydrodeoxygenation reactions.[39-41] Allegrini *et al.*[29] showed the potential of reductive deoxygenation using copper on different supports, where aromatic ketones were fully deoxygenated to their methylene analogues. More recently, Sittisa *et al.*[42, 43] reported that surface copper interacts preferentially with carbonyl groups rather than with aromatic rings. This was explained in terms of the preferred adsorption mode on Cu, η^1(O)−carbonyl, and the relatively weak interaction of copper with carbon-carbon double bonds.[42] Therefore, we reasoned that copper sites might help to retain the aromaticity of our products. In terms of supports, we used the acidic/basic combination of magnesia-alumina (details of which are in Chapter 3 and published elsewhere)[44] and pure γ–alumina. We thus synthesised CuO/γ−Al_2O_3 and CuO/MgO−Al_2O_3 by impregnation with $Cu(NO_3)_2$.

The X-ray diffraction patterns of Cu/γ−Al_2O_3 and CuO/γ−Al_2O_3 show broad peaks for the alumina, indicating lack of crystallinity of the sample. This is consistent with the literature.[45] However, the copper peaks are very sharp, which suggests the presence of large Cu clusters (at least 5-10 nm, Figure 1). Using TPR data (see Figure 2) to approximate the reduced metal content by measuring the hydrogen consumption, we calculated that there was 10.6 wt% of copper on the alumina and 10.4 wt% of copper on magnesia-alumina. Nonetheless, two main differences can be observed when comparing the two graphs: the peak shape and the temperature of reduction. In Cu/γ−Al_2O_3, we can identify two peaks and a temperature of reduction ranging from 230 to 250 °C. Both peaks correspond to the reduction of Cu(II). The first peak is assigned to highly dispersed copper oxide species, whilst the second one is a bulk-like CuO phases, including large clusters CuO particles on the γ−Al_2O_3 surface.[46]

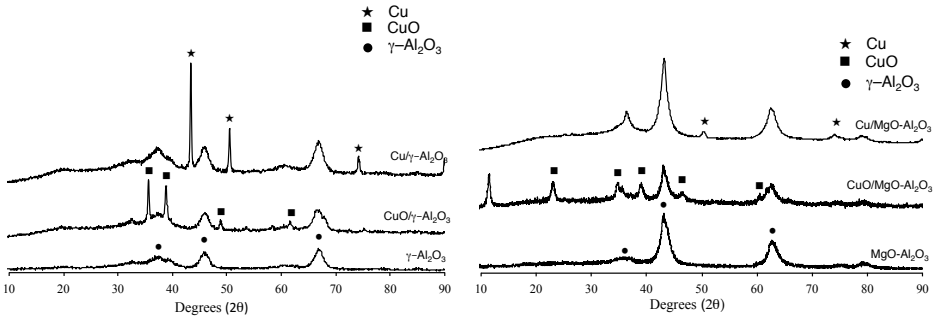

Fig. 1: X-ray diffraction patterns of CuO/γ−Al_2O_3 and Cu/γ−Al_2O_3 (left) and CuO/MgO−Al_2O_3 and Cu/MgO−Al_2O_3 (right).

In the case of Cu/MgO−Al_2O_3, the reduction temperature was higher than for CuO/γ−Al_2O_3 (see Figure 2). This indicates a stronger interaction between copper oxide and the MgO−Al_2O_3 support, hindering the reduction of Cu. This is in line with the temperature needed for calcination: 500 °C (2 °C/min) for 4 h.[47]

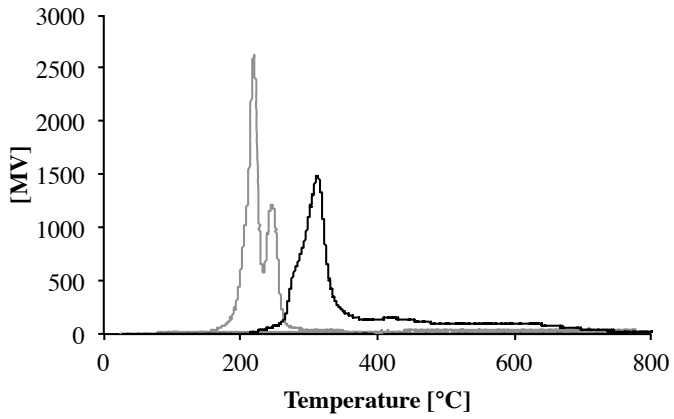

Fig. 2: Temperature programmed reduction (TPR) plots for CuO/γ–Al_2O_3 (gray line) and CuO/MgO–Al_2O_3 (black line) using hydrogen as reducing agent.

4.2.2. Screening of copper catalysts

In a typical reaction (eq 3), a solution of 2−phenoxy−1−phenylethanone **1** or 2−phenoxy−1−phenylethanol **2** in ethyl acetate was stirred under 25 bar of H_2 at 150 °C with 2 wt% unreduced catalyst (see detailed procedure in the experimental section). To investigate the possible role of Cu(0), the catalyst was also introduced after pre-reducing in H_2 for 2 h at 300 °C (the reduction temperature was selected on the basis of TPR results, see figure 2). Reaction progress was monitored by GC. Note that obtaining a quantitative mass balance in HDO reactions is particularly difficult.[32] Here we succeeded in quantifying typically 85–95% with careful calibration and rigorous low-temperature quenching of the reaction mixture.

The main products were monoaromatics, (see tables 1 and 2) plus typically 3–18% of oligomers. When using the ketone **1**, we also observed a significant amount of reduction to the alcohol **2**. Using Cu/γ−Al_2O_3 and Cu/MgO−Al_2O_3 gives phenol and ethylbenzene as the main monoaromatic products. This indicates that the cleavage occurs mostly at the C–O−aryl bond (pathway ***B*** in Scheme 2) and that HDO is the main reaction route. Introducing basic sites on the support hinders HDO and the selectivity to ethylbenzene drops considerably (see for example the last two entries in table 1 and 2).

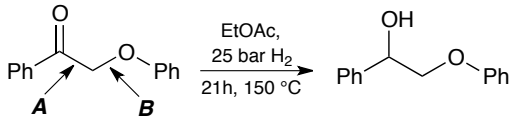

(3)

+ PhOH + PhCOMe + PhOMe + PhCHO

3	**4**	**5**	**6**
14%	5%	0%	2%

+ PhCOOH + PhC2H4OH + PhEt + oligomers

7	**8**	**9**	
0%	<1%	21%	13%

Table 1: Product distribution in the conversion of 2−phenoxy−1−phenylethanol **2**

Catalyst	**Reactant**	**Conv. %**	**Mass Balance %**	**3**	**5**	**8**	**9**	**Olig.**
				Yield %[a)]				
no catalyst	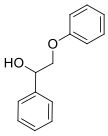	< 2	98.0	< 1	0	0	0	< 1
γ−Al_2O_3		25.7	89.5	2.5	0.4	1.5	0	18.2
MgO−Al_2O_3		23.4	94.8	5.0	0.4	3.9	0	11.8
CuO/γ−Al_2O_3[b)]		16.8	95.6	3.6	0.4	9.7	2.4	8.7
CuO/MgO−Al_2O_3[b)]		20.6	87.5	10.9	0	4.1	0	2.6
Cu/γ−Al_2O_3[c)]		52.5	93.0	21.7	0.1	2.4	19.1	5.2
Cu/MgO−Al_2O_3[c)]		47.0	95.0	24.7	0.1	1.3	8.3	9.1

[a)] Yields determined by GC analysis (chlorobenzene is the external standard).
[b)] Standard reaction conditions: 0.120 mg reactant **2** in10 mL EtOAc; 25 bar H_2; 150 °C; 21 h, 2 wt% catalyst (amount of copper relative to **2**) and with a minimal TON of 8-10. Catalyst was used without prior reduction and no inert conditions during reaction process.
[c)] Standard reaction conditions: 0.120 mg reactant **2** in 10 mL EtOAc; 25 bar H_2; 150 °C; 21 h, 2 wt% catalyst (amount of copper relative to **2**) and with a minimal TON of 23-26. Prior to the experiments, all catalysts were reduced at 300 °C under a flow of H_2 for 2 h, the solvent was purged for 2 h with N_2 and autoclaves were purged twice with pure H_2.

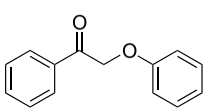
1

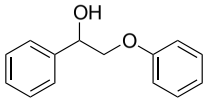
2

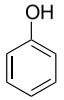
3

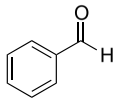
4

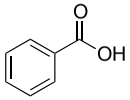
5

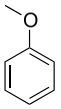
6

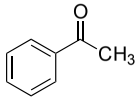
7

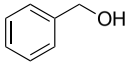
8

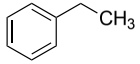
9

Table 2: Product distribution for the conversion of 2−phenoxy−1−phenylethanone **1**

Catalyst	Reactant	Conv. %	Mass Balance %	**2**	**3**	**4**	**5**	**6**	**7**	**8**	**9**	oligomers
				Yield %[a]								
no catalyst	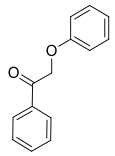	4.71	95.3	0.0	3.3	0.0	0.0	0.0	0.0	0.0	0.0	0.9
$\gamma-Al_2O_3$		38.7	91.4	0.0	18.8	0.5	0.4	1.2	6.6	0.0	0.0	7.8
$MgO-Al_2O_3$		30.0	89.0	0.0	12.2	0.6	0.6	4.3	2.6	0.0	0.0	5.6
$CuO/\gamma-Al_2O_3$[b]		96.7	88.1	45.2	17.3	1.8	0.7	1.9	9.1	2.2	0.0	6.1
$CuO/MgO-Al_2O_3$[b]		99.1	94.4	50.3	9.5	5.6	0.5	0.0	8.5	0.6	0.0	18.1
$Cu/\gamma-Al_2O_3$[c]		97.7	81.5	24.5	14.1	5.1	0.0	0.0	0.0	0.6	21.9	13.6
$Cu/MgO-Al_2O_3$[c]		82.3	87.5	34.4	10.2	1.6	0.1	4.3	0.0	4.3	5.3	16.3

[a] Yields determined by GC analysis (chlorobenzene is the external standard).
[b] Standard reaction conditions: 0.120 mg reactant **1** in10 mL EtOAc; 25 bar H_2; 150 °C; 21 h, 2 wt% catalyst (amount of copper relative to **1**) and with a minimal TON of 48-50. Catalyst was used without prior reduction and no inert conditions during reaction process.
[c] Standard reaction conditions: 0.120 mg reactant **1** in10 mL EtOAc; 25 bar H_2; 150 °C; 21 h, 2 wt% catalyst (amount of copper relative to **1**) and with a minimal TON of 42-48. Prior to the experiments, all catalysts were reduced at 300 °C under a flow of H_2 for 2 h, the solvent was purged for 2 h with N_2 and autoclaves were purged three times.

Interestingly, the alcohol **2** is less reactive than its ketone counterpart. Other studies on several β−O−4 models reported a reduction of the bond dissociation energy (BDE) for oxidized species compared to their alcohol analogues.[48, 49] We calculated BDEs with DFT for our reactants as well, showing that indeed the ether bond is weaker in the ketone than in the alcohol (table 3). As BDEs only explain the thermal non-catalytic cleavage, we also studied the cleavage of protonated molecules (the cleavage is catalysed by alumina, the activity of which is usually explained by its acidity). However, these calculations were severely hindered by reorganisation of bonds, and therefore no numbers are reported here. We do observe that for both, the ketone and the alcohol, the ether bond (pathway ***B*** in Scheme 2) is activated by protonation. In case of the alcohol, an immediate reorganisation occurs resulting in oligomerisation rather than cleavage. This fits strikingly well with the oligomerisation observed experimentally.

Table 3: Bond dissociation energies (BDEs) of **1** and **2** for pathways **A** and **B**.

Reactant	Pathway	BDE (kJ/mol)
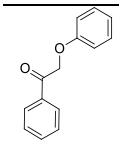	**A**	265
	B	253
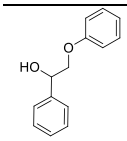	**A**	284
	B	201

The three-dimensional shape/confirmation and bond rotations of the molecules could also be playing a role in the difference in reactivity between the alcohol and ketone. Modelling the ketone and the corresponding alcohol in the gas phase, we see that the ketone (sp^2 carbon and oxygen bound by π) is planar, which allows for both oxygens to adsorb simultaneously (see Figure 3). In the alcohol, however this bond can rotate freely (sp^3 carbon and oxygen bound by σ) and, as a consequence, the molecule adsorbs twisted (see Figure 3) making adsorption more difficult. In fact, constraining the alcohol into a planar shape would require an extra 12 kJ/mol.

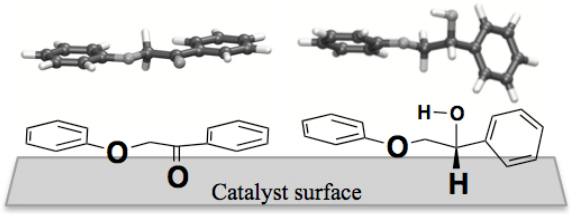

Fig. 3: DFT–optimised 3D structures of the ketone **1** (top left) and the alcohol **2** (top right) and a possible approach of these to the catalyst surface (bottom).

Nichols *et al.*[50] reported the oxidation of the alcohol dimer **2** to the ketone dimer **1** via a well-known Ru–dehydrogenative equilibrium. In our conditions (substrate **2** and 25 bar of hydrogen pressure), this equilibrium is not observed, as neither dimer **1** nor acetophenone **4** were detected by GC analysis. To rule out the influence of the thermal cleavage in absence of hydrogen, we ran a series of control experiments with argon. These reactions gave less than 5% conversion. The main products were high-molecular-weight oligomers, with no oxidation of dimer **2** to dimer **1**. Thus, 150 °C and an external hydrogen source are required to cleave the β−O−4 linkage via hydrogenolysis. A series of blank experiments starting from **1**, both in absence of catalyst and with the bare support, showed no traces of the alcohol **2** either. This confirms that the reduction of **1** to **2** requires the presence of copper in the active site.

For both, **1** and **2**, we envisage a two-step process. To illustrate this hypothesis, we propose the following mechanism for dimer **1** (Scheme 2). Alumina-catalysed hydrogenolysis of the dimer's C–O(aryl) bond (pathway **B**) occurs first, giving acetophenone and phenol. This is followed by copper-catalysed hydrodeoxygenation of the carbonyl group to the corresponding ethylbenzene. The presence of benzaldehyde and anisole can be explained by the hydrogenolysis of the OC–CH_2O(aryl) bond (pathway **A**). Then, benzaldehyde is rapidly oxidized by air to benzoic acid (the latter is indeed absent under inert conditions, confirming that oxygen is needed[51]). If both bonds **A** and **B** are cleaved, methane may form. For dimer **1,** the hydrogenation of the ketone can occur as a third pathway when Cu or CuO is present. Dimer **2** can also split under influence of the alumina, but this only leads to oligomerisation. When metallic copper is present, dimer **2** can be converted to phenol and **8**. This explains the smaller amount of dimer **2** in the product mixture when starting from **1** and using the Cu/Al_2O_3 catalyst.

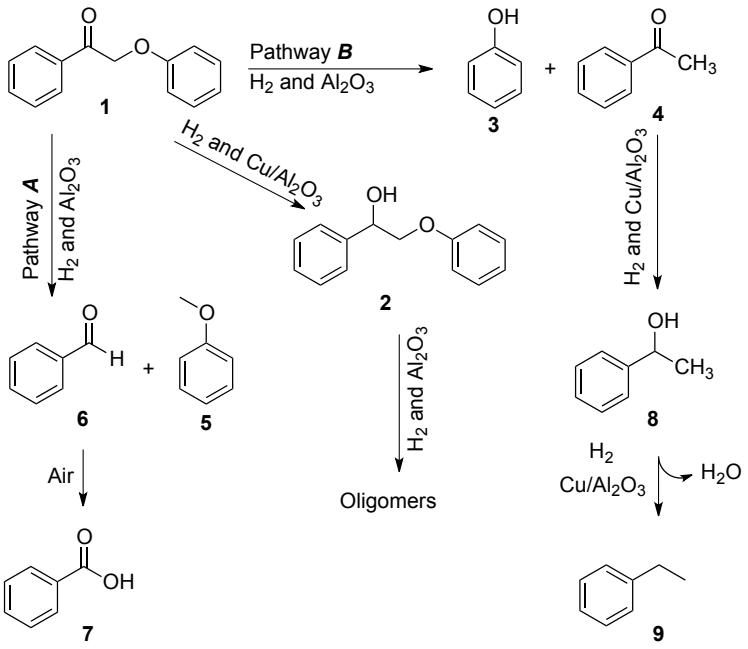

Scheme 2: Proposed mechanism for the β–O–4 cleavage of dimer **1**.

Notably, up to 22% yield of ethylbenzene was identified using a reduced copper catalyst and removing air/oxygen from the reaction mixture (see experimental procedure for both **1** and **2**). This is in agreement with the two-step route outlined above. The experiments gave approximately proportional yields of phenol and ethylbenzene for both **1** and **2**. Looking at the XRD pattern, we conclude that HDO occurs more readily with larger copper agglomerates than on finely dispersed sites.[52] The highest selectivity towards phenol and ethylbenzene is obtained using plain alumina as a support, which also has the largest copper clusters. In contrast, when we used unreduced catalysts, copper is involved mainly in the reduction of **1** to **2**, with only traces of HDO. In the absence of HDO, some phenol is still formed by the first reaction step, namely the hydrogenolysis of the C–O aryl bond ***B***. In this case, products **4**, **5** and **7** are formed in higher amounts.

To understand the stability of our catalyst, we performed a series of recycling and leaching tests with the unreduced catalyst. The conversion remains constant after filtering the catalyst out, showing that the catalyst does not leach into solution. However, in the recycling experiments the conversion dropped to 44% after the first cycle, indicating some degree of catalyst deactivation. Rao *et al.*[53] studied the deactivation of several copper catalysts in the hydrogenation of aromatic ketones and aldehydes. They reported that the catalyst deactivation occurs via different pathways: coke formation and/or poisoning of the catalyst (by product adsorption), or a change in the oxidation state of the copper during the reaction. Twigg and Spencer[54] studied the deactivation of supported copper metal catalysts for different hydrogenation reactions. They highlighted four main causes: (i) coke formation, (ii) sintering of copper particles, (iii) change in the oxidation state of copper and (iv) catalyst poisoning by chlorine or sulfur compounds or adsorbed by-products on the catalyst. Under our stated reaction conditions, poisoning of the catalyst with sulfur or chlorine is unlikely. The reaction temperatures are too low to involve sintering. Because we have organic hydrogenation reactions, coking is the more plausible explanation. Considering the close chemical similarity with our reaction products, similar deactivation processes may occur in the conversion of **1** and **2**.

4.3. Conclusion

Copper particles supported on γ–alumina catalyse the scission of β−O−4 linkages under HDO conditions, yielding phenol and ethylbenzene in substantial amounts. Using magnesia-alumina as the support increases the dispersion of copper, yet lowers the selectivity towards HDO. For industrial applications, the catalyst price/performance ratio is a key criterion, and the main challenge in this case is catalyst stability. Working with real lignin depolymerisation feeds means dealing with sulphur in the feedstock, as well as rapid deactivation by coke formation and potential poisoning by water. Importantly, our supported copper catalysts are cheap and readily available. As such, they open a practical route for decreasing the oxygenated content of lignin model compounds streams while keeping the aromatic rings intact, a key hurdle for efficient biomass conversion.[55]

4.4. Experimental section

4.4.1. Materials, instrumentation and computational methods

Unless otherwise specified, all chemicals were purchased from commercial sources and used as received. The $MgO-Al_2O_3$ was provided by Eurosupport.[56] X−Ray diffraction (XRD) patterns were obtained with a MiniFlex II diffractometer using Ni−filtered CuKα radiation. The X-ray tube was operated at 30 kV and 15 mA. Temperature programmed reduction (TPR) was carried out using hydrogen on an instrument equipped with a thermal conductivity detector (TCD). Samples of *ca.* 100 mg were loaded into a quartz U-tube reactor and where pre-treated in N_2 (40 ml/min) at 473 K for 30 min. After cooling to ambient temperature, the gas stream was switched to 5 % H_2/N_2 flowing at 40 ml/min. The samples were heated at 10 K/min to 1000 K, during which the hydrogen consumption was monitored by TCD. Quantification of H_2 content was based on detailed calibration of H_2 injections in the same reduction stream. Surface area measurements were performed by the BET method using N_2 at 77 K on a Thermo Scientific Surfer instrument. The samples were dried in vacuum (1×10^{-3} mbar) for 3 h at 200 °C prior to the measurement. Gas chromatography analyses were run on an Interscience GC−8000 gas chromatograph with 14 % cyanopropylphenyl and 86 % dimethyl polysiloxane capillary column (Rtx-1701, 30 m; 25mm ID; 1μm df). Samples were diluted in 1 ml MeOH. GC conditions: isotherm at 50 ºC (2 min); ramp at 2 ºC min^{-1} to 70 ºC; ramp at 70 ºC min^{-1} to 140 ºC; ramp at 10 ºC min^{-1} to 280 ºC; isotherm at 260 ºC (2 min). Products were identified by comparing their retention times to those of authentic samples.

4.4.2. Catalyst synthesis

10 wt% CuO/γ−Al₂O₃ was synthesized by adding 1.0 g of $\gamma-Al_2O_3$ to a solution of $Cu(NO_3)_2\cdot6H_2O$ (0.38 g, 1.6 mmol) in 20 ml water and stirred for 2 h at 25 °C . The liquid was evaporated overnight on an oil bath at 60 °C, yielding a light green powder. This was dried at 120 °C for 24 h and then calcined in air at 500 °C (2 °C/min) for 4 h. The analogous *10 wt% CuO/MgO−Al₂O₃* was prepared as above starting from 1.0 g of *γ*−Al_2O_3.

4.4.3. Synthesis of 2-phenoxy-1-phenylethanone (1)

This is a modification of a previously published procedure.[37, 59] Bromoacetophenone (9.0 g, 45 mmol) and phenol (5.0 g, 53 mmol) were dissolved in 200 ml DMF, mixed with KOH (3.0 g, 53 mmol) and stirred overnight at room temperature. The product was then extracted with H_2O and Et_2O, dried over Na_2SO_4 and recrystallized from ethanol (yellowish powder, 86 mol% pure product yield based on bromoacetophenone). ^{1}H NMR (DMSO) δ 5.58 (s, 2H), 6.93–6.98 (m, 3H), 7.27–7.31 (m, 2H), 7.56–7.60 (m, 2H), 7.68–7.72 (m, 1H), 8.02–8.04 (m, 2H).

4.4.4. Synthesising of 2-phenoxy-1-phenylethanol (2)

This is a modification of a previously published procedure.[37, 59] A solution of 2-phenoxy-1-phenylethanone **1** (2.5 g, 11 mmol) in methanol (100 ml) was treated with small portions of sodium borohydride (5.5 mmol) and stirred for 2 h. A saturated solution of ammonium sulfate (200 ml) followed by $CHCl_3$ (200 ml) was added to the reaction mixture. The organic layer was separated, washed with water (2×100 ml), dried and recrystallized from ethanol (fine white needles, 73 mol% pure compound yield based on **1**). ^{1}H NMR (DMSO) δ 4.01–4.02 (m, 2H), 4.90–4.94 (m, 1H), 5.63–5.64 (d, 1H), 6.90–6.94 (m, 3H), 7.25–7.47 (m, 7H).

4.4.5. Procedure for catalytic hydrodeoxygenation (HDO)

Experiments were carried out in a six-parallel stainless steel 75 ml autoclave. In a typical experiment without inert atmosphere and without pre-reducing the catalysts (results in tables 2 and 3), 2 wt% of catalyst (copper weight relative to starting material) was added to a solution of 2–phenoxy–1–phenylethanone **1** (0.120 g, 0.56 mmol) in 10 mL of EtOAc. The autoclave was pressurized with 25 bar H_2 and heated to 150 °C for 21 h. Then, the reactors were cooled down to room temperature using an ice bath. Liquid samples were analysed by GC using chlorobenzene as external standard.

In a second set of experiments (results shown in tables 2 and 3), we used inert purging and the catalysts were pre-reduced as follows: 1.0 g of catalyst was heated at 300 °C under a 40 ml/min H_2 for 2 h. The solvent, EtOAc, was purged for 2 h with nitrogen. 2 wt% of catalyst (copper weight related to starting material) was added to an

autoclave containing a solution of 2−phenoxy−1−phenylethanone **1** (0.120 g, 0.56 mmol) in 10 ml EtOAc. The autoclaves were flushed twice with argon, then pressurized to 25 bar H_2 and heated to 150 °C for 21 h. The reactors were cooled down to room temperature using an ice bath. Liquid samples were analysed by GC using chlorobenzene as external standard.

4.4.6. Procedure for recycling and leaching tests

Recycling and leaching tests were carried out in a six-parallel stainless steel 75 ml autoclave. For the recycling test, 2 wt% of catalyst (copper weight relative to starting material using 10 wt% $CuO/\gamma-Al_2O_3$) was added to a solution of 2−phenoxy−1−phenylethanone **1** (0.240 g, 1.12 mmol) in 20 ml of EtOAc. The autoclave was pressurized with 25 bar H_2 and heated to 150 °C for 21 h. Then, the reactors were cooled down to room temperature using an ice bath. The catalyst was filtered out and placed in a desiccator overnight. The recycled catalyst was then reused for an extra 21 h reaction using 2−phenoxy−1−phenylethanone **1** (0.120 g, 0.56 mmol) in 10 mL of EtOAc with 2 wt% of catalyst (copper weight relative to starting material). Liquid samples were analysed by GC using chlorobenzene as external standard.

For the leaching test, the autoclave was pressurized with 25 bar H_2 and heated to 150 °C for 3 h. Then, the reactors were cooled down to room temperature using an ice bath. The catalyst was filtered out and the reaction mixture (without catalyst) was charged again with 25 bar H_2 and heated to 150 °C for 20 h. Liquid samples were analysed by GC using chlorobenzene as external standard.

4.4.7. DFT calculations for the intimate pair of alcohol dimer

DFT calculations were performed with the ADF package,[57] using the rPBE functional[58] and a DZP basis set. Calculations were done on isolated molecules. BDEs were calculated by comparing the energies of the starting molecules and the isolated radicals formed. For the protonated species, linear transits were performed, slowly breaking the bonds instead of comparing only the end energy. In this way, the calculations allow to simulate oligomerisation.

An alternative explanation is that two alcohol dimers may form an intimate pair via two hydrogen bonds. This would protect the alcohol dimer from reaction. However, both theory and experiment refute this hypothesis: our DFT calculations show that the hydrogen bonds between the alcohol dimer and a solvent molecule (ethyl acetate) are much stronger (24 kJ/mol) than those between two alcohol dimers.

4.4.8. Surface area measurements (BET method)

Name	**Active species**	**Support**	**Surface area** [m^2/g]	**Pore volume** [cm^3/g]
Al_2O_3	-	Al_2O_3	193	0.46
$MgO\text{-}Al_2O_3$	-	$MgO\text{-}Al_2O_3$	175	0.45
$Cu/MgO\text{-}Al_2O_3$	10% Cu	$MgO\text{-}Al_2O_3$	166	0.26
Cu/Al_2O_3	10% Cu	Al_2O_3	140	0.35

4.5. References

1. E. Furimsky, *Appl. Catal. A.*, **2000**, 199, 147-190.

2. P. T. Vasudevan and J. L. G. Fierro, *Catal. Rev.*, **1996**, 38, 161-188.

3. R. A. Sànchez-Delgado, *Hydrodesulfurization and Hydrodenitrogenation*, Springer, Amsterdam, **2002**, 1-34.

4. A. J. Ragauskas, C. K. Williams, B. H. Davison, G. Britovsek, J. Cairney, C. A. Eckert, W. J. Frederick, J. P. Hallett, D. J. Leak, C. L. Liotta, J. R. Mielenz, R. Murphy, R. Templer and T. Tschaplinski, *Science*, **2006**, 311, 484-489.

5. T. V. Choudhary and C. B. Phillips, *Appl. Catal. A.*, **2011**, 397, 1-12.

6. E. Furimsky, *Catal. Rev. Sci. Eng.*, **1983**, 25, 421-458.

7. D. Mohan, C. U. Pittman and P. H. Steele, *Energy & Fuels*, **2006**, 20, 848-889.

8. A. Jess and P. Wasserscheid, *Chemical Technology; an Integrated Textbook.*, Wiley-VCH, Weinheim, **2013**.

9. J. Gierer, *Wood Sci. Technol.*, **1980**, 14, 241-266.

10. R. Vanholme, B. Demedts, K. Morreel, J. Ralph and W. Boerjan, *Plant Physiol.*, **2010**, 153, 895-905.

11. R. Hatfield and W. Vermerris, *Plant Physiol.*, **2001**, 126, 1351-1357.

12. E. Adler, *Wood Sci. Technol.*, **1977**, 11, 169-218.

13. F. S. Chakar and A. J. Ragauskas, *Ind. Crops Prod.*, **2004**, 20, 131-141.

14. S. Kang, L. Xiao, L. Meng, X. Zhang and R. Sun, *Int. J. Mol. Sci.*, **2012**, 13, 15209-15226.

15. J. Zakzeski, P. C. A. Bruijnincx, A. L. Jongerius and B. M. Weckhuysen, *Chem. Rev.*, **2010**, 110, 3552-3599.

16. J. B. s. Bredenberg, M. Huuska, J. Räty and M. Korpio, *J. Catal.*, **1982**, 77, 242-247.

17. J. Magano and J. R. Dunetz, *Org. Process Res. Dev.*, **2012**, 16, 1156-1184.

18. T. J. Connolly, M. Matchett, P. McGarry, S. Sukhtankar and J. Zhu, *Org. Process Res. Dev.*, **2004**, 8, 624-627.

19. J. T. Kuethe, K. G. Childers, Z. Peng, M. Journet, G. R. Humphrey, T. Vickery, D. Bachert and T. T. Lam, *Org. Process Res. Dev.*, **2009**, 13, 576-580.

20. D. Gauvreau, S. J. Dolman, G. Hughes, P. D. O'Shea and I. W. Davies, *J. Org. Chem.*, **2010**, 75, 4078-4085.

21. S.-C. Kuo, F. Chen, D. Hou, A. Kim-Meade, C. Bernard, J. Liu, S. Levy and G. G. Wu, *J. Org. Chem.*, **2003**, 68, 4984-4987.

22. H. Li, Z. Xia, S. Chen, K. Koya, M. Ono and L. Sun, *Org. Process Res. Dev.*, **2007**, 11, 246-250.

23. M. H. Yates, T. M. Koenig, N. J. Kallman, C. P. Ley and D. Mitchell, *Org. Process Res. Dev.*, **2009**, 13, 268-275.

24. P. Herold, A. F. Indolese, M. Studer, H. P. Jalett, U. Siegrist and H. U. Blaser, *Tetrahedron*, **2000**, 56, 6497-6499.

25. R. H. Mitchell and Y.-H. Lai, *Tetrahedron Lett.*, **1980**, 21, 2637-2638.

26. D. Poondi and M. A. Vannice, *J. Mol. Catal. A: Chem.*, **1997**, 124, 79-89.

27. M. A. Vannice and D. Poondi, *J. Catal.*, **1997**, 169, 166-175.

28. J. Ma, S. Liu, X. Kong, X. Fan, X. Yan and L. Chen, *Res. Chem. Intermed.*, **2012**, 38, 1341-1349.

29. F. Zaccheria, N. Ravasio, M. Ercoli and P. Allegrini, *Tetrahedron Lett.*, **2005**, 46, 7743-7745.

30. B. Coq, F. o. Figueras, P. Geneste, C. Moreau, P. Moreau and M. Warawdekar, *J. Mol. Catal.* , **1993**, 78, 211-226.

31. S. Jia, B. J. Cox, X. Guo, Z. C. Zhang and J. G. Ekerdt, *Ind. Eng. Chem. Res.*, **2010**, 50, 849-855.

32. A. L. Jongerius, R. Jastrzebski, P. C. A. Bruijnincx and B. M. Weckhuysen, *J. Catal.*, **2012**, 285, 315-323.

33. H. Kawamoto, S. Horigoshi and S. Saka, *J. Wood Sci.*, **2007**, 53, 168-174.

34. R. J. A. Gosselink, W. Teunissen, J. E. G. van Dam, E. de Jong, G. Gellerstedt, E. L. Scott and J. P. M. Sanders, *Bioresour. Technol.*, **2012**, 106, 173-177.

35. K. Takeno, T. Yokoyama and Y. Matsumoto, *BioResources*, **2012**, 7, 99-111.

36. T. vom Stein, T. Weigand, C. Merkens, J. Klankermayer and W. Leitner, *ChemCatChem*, **2012**, 5, 439-441.

37. P. F. Britt, A. C. Buchanan, M. J. Cooney and D. R. Martineau, *J. Org. Chem.*, **2000**, 65, 1376-1389.

38. J. E. Tilton and G. Lagos, *Resour. Policy*, **2007**, 32, 19-23.

39. T. T. Pham, L. L. Lobban, D. E. Resasco and R. G. Mallinson, *J. Catal.*, **2009**, 266, 9-14.

40. M. V. Bykova, D. Y. Ermakov, V. V. Kaichev, O. A. Bulavchenko, A. A. Saraev, M. Y. Lebedev and V. A. Yakovlev, *Appl. Catal. B.*, **2012**, 113-114, 296-307.

41. V. Dundich, S. Khromova, D. Ermakov, M. Lebedev, V. Novopashina, V. Sister, A. Yakimchuk and V. Yakovlev, *Kinet. Catal.*, **2010**, 51, 704-709.

42. S. Sitthisa and D. E. Resasco, *Catal. Lett.*, **2011**, 141, 784-791.

43. S. Sitthisa, T. Sooknoi, Y. Ma, P. B. Balbuena and D. E. Resasco, *J. Catal.*, **2011**, 277, 1-13.

44. Z. Strassberger, S. Tanase and G. Rothenberg, *Eur. J. Org. Chem.*, **2011**, 5246-5249.

45. M. Trueba and S. P. Trasatti, *Eur. J. Inorg. Chem.*, **2005**, 2005, 3393-3403.

46. W.-P. Dow, Y.-P. Wang and T.-J. Huang, *Appl. Catal. A.*, **2000**, 190, 25-34.

47. K. M. Lee and W. Y. Lee, *Catal. Lett.*, **2002**, 83, 65-70.

48. S. Kim, S. C. Chmely, M. R. Nimlos, Y. J. Bomble, T. D. Foust, R. S. Paton and G. T. Beckham, *J. Phys. Chem. Lett.*, **2011**, 2, 2846-2852.

49. A. Beste and A. C. Buchanan, *J. Org. Chem.*, **2011**, 76, 2195-2203.

50. J. M. Nichols, L. M. Bishop, R. G. Bergman and J. A. Ellman, *J. Am. Chem. Soc.*, **2010**, 132, 12554-12555.

51. J. R. Pound, *J. Phys. Chem.*, **1930**, 35, 1496-1497.

52. P. W. Park and J. S. Ledford, *Appl. Catal. B*, **1998**, 15, 221-231.

53. R. Rao, R. T. Baker and M. A. Vannice, *Catal. Lett.*, **1999**, 60, 51-57.

54. M. V. Twigg and M. S. Spencer, *Appl. Catal., A*, **2001**, 212, 161-174.

55. P. Gallezot, *ChemSusChem*, **2008**, 1, 734-737.

56. E. J. A. X. van de Sandt, A. Wiersma, M. Makkee, H. Van Bekkum and J. A. Moulijn, *Appl. Catal. A: General*, **1997**, 155, 59.

57. G. te Velde, F. M. Bickelhaupt, E. J. Baerends, C. Fonseca Guerra, S. J. A. van Gisbergen, J. G. Snijders and T. Ziegler, *J. Comput. Chem.*, **2001**, 22, 931-967.

58. B. Hammer, L. B. Hansen and J. K. NØrskov, *Phys. Rev. B*, **1999**, 59, 7413-7421.

59. P. H. Kandanarachchi, T. Autrey and J. A. Franz, *J. Org. Chem.*, **2002**, 67, 7937-7945.